

1 Title:

2 Embryonic rifting zone revealed by a high-density survey on the southern margin of the
3 southern Okinawa Trough

4

5 Ayanori Misawa¹ · †

6 Masahiko Sato^{1,2}

7 Seishiro Furuyama^{1,3}

8 Jih-Hsin Chang¹

9 Takahiko Inoue¹

10 Kohsaku Arai¹

11

12 1: Geological Survey of Japan, National Institute of Advanced Industrial Science
13 and Technology (AIST)

14 2: Department of Earth and Planetary Science, The University of Tokyo

15 3: Department of Marine Resources and Energy, Tokyo University of Marine
16 Science and Technology,

17

18 Corresponding author: Ayanori Misawa (ayanori-misawa@aist.go.jp)

19

20 Key Points

21 · A graben controlled by a normal fault was discovered in the southern Okinawa
22 Trough offshore northern Ishigaki-Jima Island.

23 · Magnetic anomaly and seismicity data indicate relatively shallow magma acting as
24 a heat source.

25 · The graben likely manifests an embryonic rifting on the southern margin of the
26 southern Okinawa Trough.

27 **Abstract**

28 Offshore northern Ishigaki-Jima Island, in the southern Okinawa Trough, offers
29 outstanding opportunities to explore the rifting stage of a backarc system. We report the
30 results of integrated marine geological and geophysical surveys with high-density
31 survey lines in this area. We identify a graben bounded by normal faults and extending
32 approximately 59 km in an ENE-WSW direction off-axis of the southern Okinawa
33 Trough. Submarine volcanoes with active hydrothermalism and associated intrusive
34 structures lie in the graben. Magnetic anomaly and seismicity data in and around the
35 graben suggest the presence of relatively shallow magma acting as a heat source. All
36 features identified in and around the graben suggest active rifting in the southern
37 Okinawa Trough.

38

39 **Plain Language Summary**

40 The Okinawa Trough, adjacent to the southwesternmost Japanese islands, has
41 experienced rifting of its continental crust since 2Ma. The southern part of the Trough
42 includes a rift valley, the Yaeyama Rift, where rifting is active. Herein, using marine
43 geological and geophysical data, we report the discovery of a graben bounded by
44 normal faults on the southern margin of the southern Okinawa Trough. The graben
45 hosts several submarine volcanoes, under which magnetic anomalies suggest relatively
46 shallow magma. Because these geologic features resemble graben in the axial trough,
47 we propose that the newly identified graben represents a rifting episode previously
48 undocumented for the geological evolution of the Okinawa Trough.

49

50

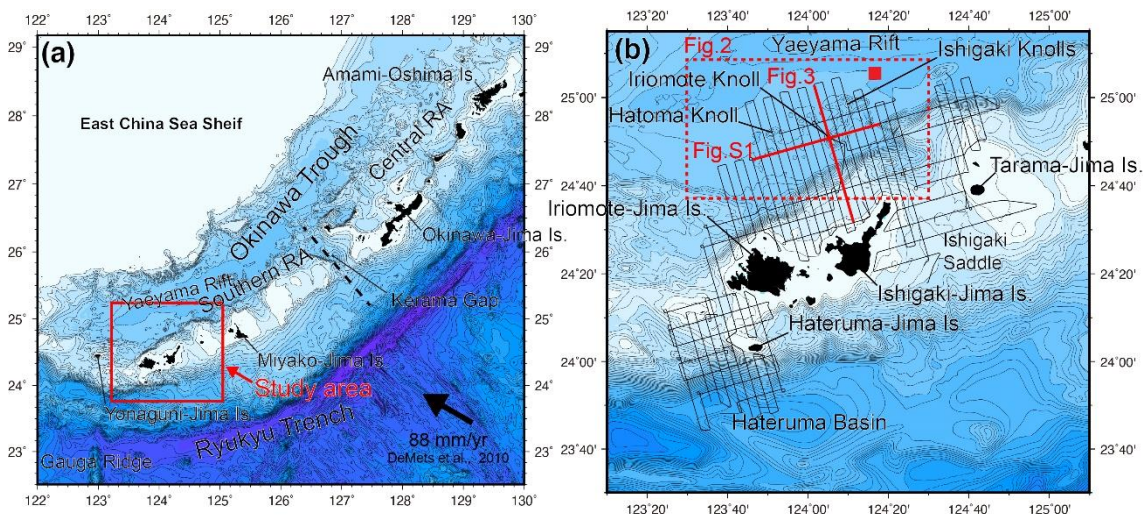
51 Keywords:

52 Okinawa Trough, Backarc basin, Normal fault, Graben, Submarine volcano

53 **1. Introduction**

54 Backarc basins on continental margins are important constituents of the plate tectonic
55 paradigm, and knowledge of their evolution is key to understanding the development of
56 the lithosphere. A backarc system typically evolves from rifting to seafloor spreading.
57 Compared to seafloor spreading, rifting on continental margins is not well understood
58 due to the current rarity of such deformations. Among backarc basins located on
59 continental margins, the Okinawa Trough (OT) is unique in that the backarc system is
60 actively rifting, but no seafloor spreading has occurred (e.g., Lee et al., 1980; Raju et al.,
61 2004; Keller et al., 2002; Jourdain et al., 2016). Intermittent rifting of the OT has been
62 occurring since 2 Ma (e.g., Sibuet et al., 1987; 1995; 1998).

63



64

65 **Figure 1** Tectonic map of the south Okinawa Trough area. (a) Bathymetry of the
66 Ryukyu Island arc. The inset shows the main study area offshore northern
67 Ishigaki-Jima Island. Black arrows indicate Philippine Sea plate motions
68 (DeMets et al., 2010). Dashed black lines indicate the position of the Kerama
69 Gap, which is deemed to be the boundary between the Southern Ryukyu Arc
70 and the Central Ryukyu Arc (Konishi, 1965). (b) Bathymetry offshore

71 northern Ishigaki-Jima Island and GH18 cruise survey lines. Bold red lines
72 indicate seismic profiles used in this study. The red square represents the
73 position of a magma chamber (Arai et al. 2017). Both bathymetric maps used
74 JTOPO30 grid data. RA: Ryukyu Arc.

75

76 The area offshore northern Ishigaki-Jima Island, located in the southern OT, is ideal
77 for investigating rifting of a backarc system on a continental margin (Fig. 1). Previous
78 seismic refraction surveys show no evidence of basaltic crust associated with seafloor
79 spreading (e.g., Hirata et al., 1991; Nakahigashi et al., 2004), and numerous submarine
80 volcanos suggest active magmatism associated with OT rifting (e.g., Sibuet et al., 1987;
81 1995; 1998). Among the submarine volcanoes, hydrothermal activity has been observed
82 at Hatoma Knoll, the Yonaguni Knoll *IV* field, and Yaeyama Knoll on the trough axis
83 (e.g., Toki et al., 2016; Konno et al., 2006; Miyazaki et al., 2017).

84 To investigate the geological structure along the island arc and the southern margin of
85 the OT, an integrated marine geological and geophysical survey with high-density lines
86 was conducted offshore northern Ishigaki-Jima and Hateruma-Jima islands (Fig. 1b).
87 We report on newly discovered embryonic rift features offshore northern Ishigaki-Jima
88 Island in the OT.

89

90 **2. Geological setting**

91 The Ryukyu subduction system consists of the Ryukyu Trench, the Ryukyu arc, and
92 the OT, and is a typical trench-arc-backarc system (Fig. 1a). In the Ryukyu Trench, the
93 Philippine Sea (PHS) plate is obliquely subducting beneath the Eurasian plate. The
94 subduction rates of the plates differ in the northern and southern parts of the arc region,

95 and the PHS plate subducts at 88 mm/yr in the southern OT (DeMets et al., 2010).
96 Major components of the Ryukyu Islands are considered to be a forearc (outer arc) high,
97 composed of pre-Cretaceous high-pressure metamorphic rocks, Eocene volcanic rocks,
98 and Miocene sediments (Kizaki, 1976; Letouzey and Kimura, 1986). Various theories
99 have been proposed for the timing of southern OT backarc rifting. Sibuet et al. (1987)
100 suggested that the first phase of rifting occurred after a major early Miocene change in
101 PHS plate motion with respect to Eurasia, and ceased during the Pliocene. Subsequently,
102 a second rifting phase started at the Plio-Pleistocene transition and has continued to the
103 present (Sibuet et al. 1987). In contrast, Miki (1995) proposed a two-phase opening
104 model, the first phase lasting from 10 to 6 Ma, and the second occurring at ~1 Ma.
105 Seismic data from the Yaeyama Rift in the OT axis indicates active rifting (Lee et al.,
106 1980). On the basis of seismic profiles from the Yaeyama Rift, Arai et al. (2017) and
107 Nishizawa et al. (2019) interpreted normal faults bounding the Yaeyama Rift and the
108 stratigraphy of well-stratified trough-fill sediments. Arai et al. (2017) identified a less
109 reflective zone and a low-velocity zone in the trough-fill sediments, and suggested the
110 presence of an off-axis magma chamber in the OT (Fig.1b). Southwards, several knolls
111 are distributed in the OT offshore northern Ishigaki-Jima Island, including the Ishigaki
112 Knolls, Minna Knoll, Iriomote Knoll, Daini-Kobama Knoll, Daiichi-Kobama Knoll,
113 Hatoma Knoll, and the Hatoma Hill Chain (Fig. 2a). These knolls are reported to be
114 submarine volcanos (Watanabe et al., 1995).

115

116 **3. Method and materials**

117 We conducted integrated marine geological and geophysical surveys around
118 Ishigaki-Jima Island in the Ryukyu Islands using research vessel (R/V) *Hakurei*

119 operated by the Japan Oil, Gas and Metals National Corporation (JOGMEC) in August
120 2018. We acquired high-resolution multi-channel seismic (MCS) reflection, multi-beam
121 echo sounder (MBES) swath bathymetry, sub-bottom profiler, gravity, and magnetic
122 field data. Survey line spacings were 2 nautical miles (nm) in the NNW-SSE direction
123 and 4 nm in the WSW-ENE direction (Fig. 1b). Combined, these data illuminate the
124 geological structure offshore northern Ishigaki-Jima Island.

125 The seismic source was a GI gun (*Sercel*) comprising a total volume of 355 cubic
126 inches (G: 250 cubic inches; I: 105 cubic inches). The shot interval of 6.1 s
127 corresponded to ~25 m at a ship speed of ~8 knots. The receiver array used a 200
128 m-long, 32-channel solid digital streamer with group intervals of 6.25 m. The recording
129 length was 5.9 s and the sampling rate was 2.0 ms. GPS data were used for positioning.
130 Digital data were recorded with a CNT-2 seismic system (*Geometrics Inc.*) and then
131 saved in SEG-D format on board. The SEG-D format data were subsequently converted
132 to SEG-Y format, and the following data processing was performed using Seismic
133 Processing Workshop (SPW) software (*Parallel Geoscience Corp.*): common-mid point
134 (CMP) sorting, trace editing, bandpass filtering, gain recovery, deconvolution, velocity
135 analyses, normal moveout (NMO), and CMP stack.

136 Bathymetric data were collected with a multi-beam echo sounding system (EM122,
137 *Kongsberg Maritime AS*) at an operating frequency of 12 kHz from R/V *Hakurei*.
138 Additional EM122 data were acquired from R/V *No.1 Kaiyo-Maru*. Sound velocity
139 correction used real-time data from a surface water velocity meter, and sound velocity
140 profiles from conductivity, temperature, and depth instruments (CTD) and expendable
141 CTDs (XCTD) during the MBES observations. HIPS and SIPS software (*CARIS, Ltd.*)
142 was used to edit the raw bathymetry data.

143 Total magnetic field data were acquired at 0.1-s intervals with a surface-towed
144 cesium magnetometer (G-882, *Geometrics Inc.*). The sensor was towed 300 m behind
145 the ship to minimize magnetization effects from the ship. Magnetic anomalies were
146 calculated by subtracting the 13th Generation International Geomagnetic Reference
147 Field (IGRF-13) from the observed magnetic field intensity. Magnetic diurnal variation
148 was corrected using data from the Gesashi magnetic observatory on Okinawa-Jima
149 operated by the Geospatial Information Authority of Japan. Crossover error, assumed to
150 be mainly caused by ship magnetization, was minimized by using the Generic Mapping
151 Tools software package x2sys (Wessel, 2010).

152

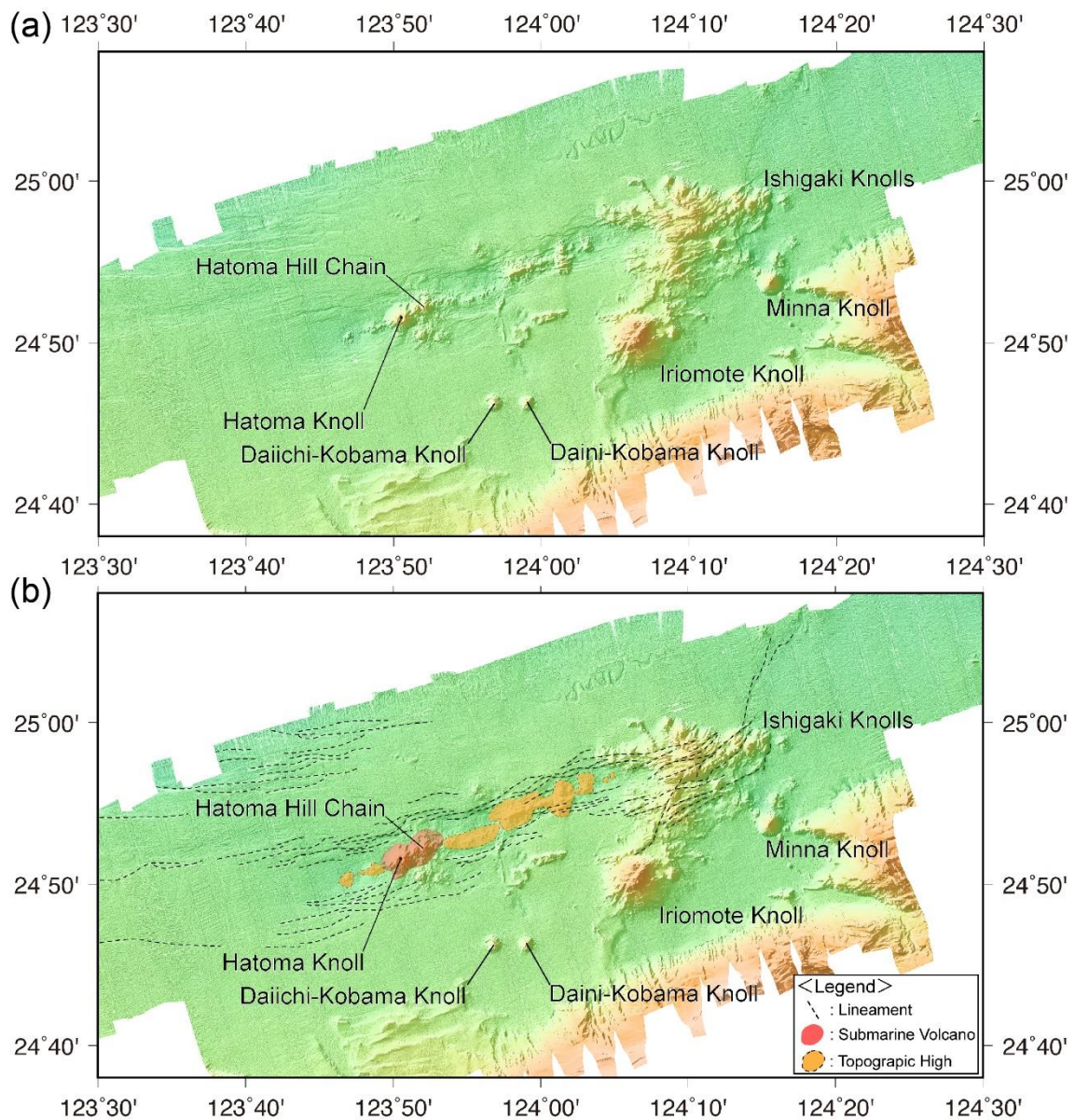
153 **4. Results**

154 **Bathymetry data**

155 The detailed seafloor morphology offshore northern Ishigaki-Jima Island obtained
156 from the two survey cruises reveals numerous knolls and seafloor lineaments trending
157 ENE-WSW (Fig. 2). An elongated depression between Hatoma Knoll and the Ishigaki
158 Knolls is bounded by two rows of ENE-WSW-trending lineaments (Fig. 2). We
159 interpret these lineaments as active faults bounding a developing graben. The graben is
160 ~59 km long and 6–10 km wide, with a maximum depth of ~100 m. These lineaments
161 likely extend across to the Ishigaki Knolls, located on the eastern side of the graben.
162 Knolls and topographic highs inside the graben (Fig. 2b) are consistent with a regional
163 interpretation of submarine volcanoes (Watanabe et al., 1995). Hatoma Knoll,
164 characterized by active hydrothermal activity, is a submarine volcano within the graben
165 (Fig. 2).

166

167



168

169 **Figure 2** New high-resolution bathymetric map offshore northern Ishigaki-Jima Island.

170 (a) Bathymetric maps were created using 20-m grid data from the two cruises.

171 (b) Morphological interpretation. This new high-resolution bathymetric map

172 reveals the ENE-WSW trending lineaments and an elongated depression

173 between the Hatoma Knoll and Ishigaki Knolls. The dashed black lines are

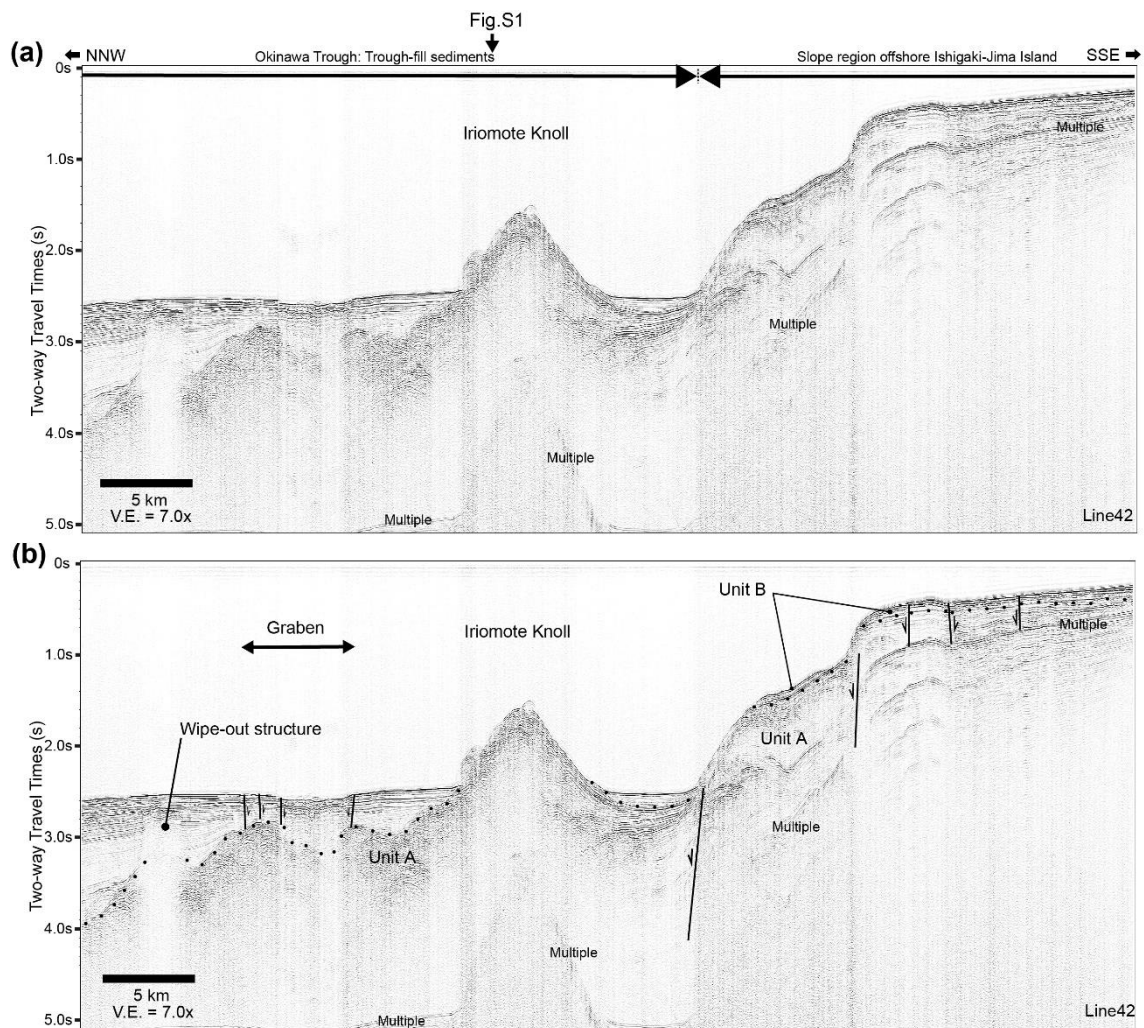
174 lineaments interpreted from the bathymetry.

175

176 **Seismic profiles**

177 Based on our seismic data, the sedimentary sequence of the OT is roughly divided
178 into Unit A and overlying trough-fill sediments, with an unconformity (Fig. S1). Unit A
179 is found from the slope region of the island arc to the OT. It seems the stratification of
180 Unit A gradually increases up-section. The seafloor observation via Remotely Operated
181 Vehicle (ROV) in this slope region confirmed that the exposed outcrop of Unit A is
182 composed of siltstones. Thus, we consider Unit A to be as a stratified sedimentary
183 sequence that partially extends from the island arc to the OT. The internal structure of
184 the trough-fill sediments is characterized by continuous, high-amplitude parallel
185 reflectors, onlapping Unit A. The thickness of the trough-fill sediments has a two-way
186 travel (TWT) time of 1.3 seconds (Fig. 3). In the NNW-SSE seismic profile (Fig. 1b),
187 the thickness of the trough-fill sediments generally increases toward the Yaeyama Rift
188 (Fig. 3). Our seismic data also show that the internal structure of the Iriomote and
189 Minna Knolls is characterized by a chaotic structure, seemingly associated with
190 submarine volcanic process. It seems possible that the structure resulted from igneous
191 intrusion and magma emplacement into Unit A and the trough-fill sediments. In
192 addition, some sections of the trough-fill sediments show chaotic patterns indicating
193 disturbance (Fig. S1). Furthermore, the unconformity is interrupted immediately
194 beneath the chaotic structure, also suggesting that the chaotic pattern results from
195 igneous intrusion and magma emplacement.

196



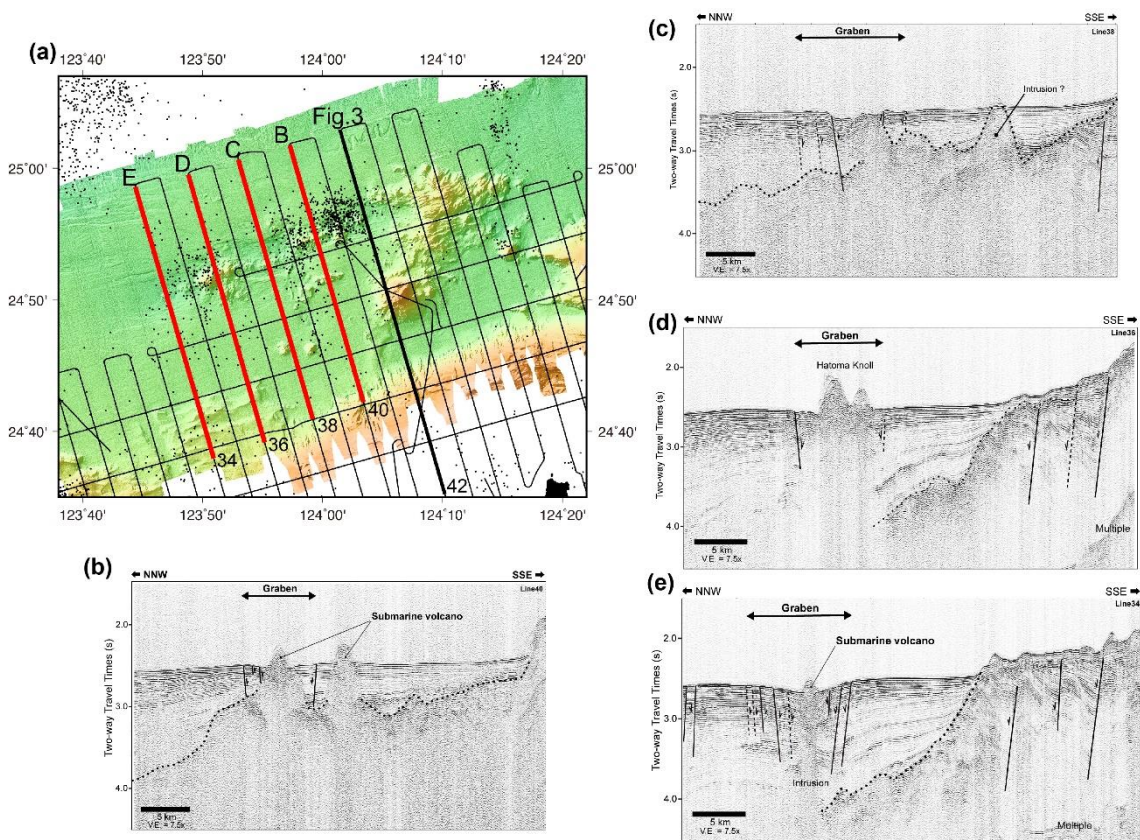
197

198 **Figure 3** Stacked seismic profile of the Okinawa Trough and backarc slope offshore
 199 northern Ishigaki-Jima Island. (a) Stacked seismic profile of MCS Line42. (b)
 200 Interpreted seismic profile. This profile shows sedimentary sequences (Unit A,
 201 Unit B, and trough-fill sediments) across the graben and wipe-out structure in
 202 the OT. Unit A is characterized by the stratified internal reflector gradually
 203 increasing up-section. Unit B is characterized by the continuous
 204 high-amplitude stratified internal reflector, while it is limited within the
 205 upslope area. The trough-fill sediments of the OT are characterized by
 206 continuous high-amplitude parallel stratified internal reflectors. The locations

207 of the profiles are shown in Fig. 1b. The dotted line indicates the
208 unconformity surface. VE is calculated using $V_p = 1,500$ m/s.

209
210 Northward-dipping normal faults dominate the slope region, and northward-dipping
211 and southward-dipping normal faults have developed in the trough-fill sediments of the
212 OT (Fig. 3). Most normal faults offset the seafloor: the vertical offsets of the northern
213 and southern bounding faults are estimated to be ~25 m and ~20 m, respectively (Fig.
214 S2). The positions of these normal faults coincide with the lineaments flanking the
215 graben (Figs. 3 and 4), indicating that the normal faults control graben formation (e.g.,
216 Lee et al., 1980; Lizarralde et al., 2007). Several intrusive structures within the graben
217 coincide with topographic highs (Fig. 4), indicating a causal relationship.

218



219

220 **Figure 4** Seismic profiles across the graben. (a) Bathymetric map showing survey lines.
221 Bathymetric maps were created using 20 m grid data. Black dots show
222 epicenters determined by the Japan Meteorological Agency (JMA) (1998 -
223 April 2018). Hypocenter depths range from 0 to 20 km, but uncertainties are
224 large due to the limited number of seismic stations around the OT. Note that
225 seismic activity is concentrated around Hatoma Knoll and the topographic
226 highs inside the graben. (b) (c) (d) and (e) Interpreted stacked seismic profile
227 of Lines 40, 38, 36, and 34, respectively. The graben is recognizable in
228 several seismic profiles. In addition, several intrusive structures are
229 recognized inside the graben, and submarine volcanos is formed due to these
230 intrusions. Dotted lines in the interpreted profiles indicate the unconformity
231 surface. VE is calculated using $V_p = 1,500$ m/s.

232

233 At the western margin of the Ishigaki Knolls, a vertical zone is acoustically
234 transparent with comparatively weak reflectors in part of the trough-fill sediments (Fig.
235 3). This feature is interpreted as a wipe-out structure, which commonly indicates the
236 presence of fluid and/or gas, or of mud diapirs (e.g., Dillon et al., 1993, Bouriak et al.,
237 2000, Sager et al., 2003, Hornbach et al., 2007). The wipe-out structure at the western
238 margin of the Ishigaki Knolls occur within the trough-fill sediments and does not reach
239 the seafloor. Its structure is characterized by a high-amplitude reflector at its top, and its
240 base is not recognizable (Fig. S3b). The high-amplitude reflector has negative-polarity,
241 the opposite of the polarity of the seafloor (Fig. S3d). These characteristics indicate the
242 presence of gas and/or fluid (e.g., Shipley et al., 1994). The wipe-out structure lies
243 within the trough-fill sediments (Fig. S3b), suggesting pervasive gas and/or fluid. In
244 addition, a flare (acoustic water column anomaly) emanating from the seafloor above

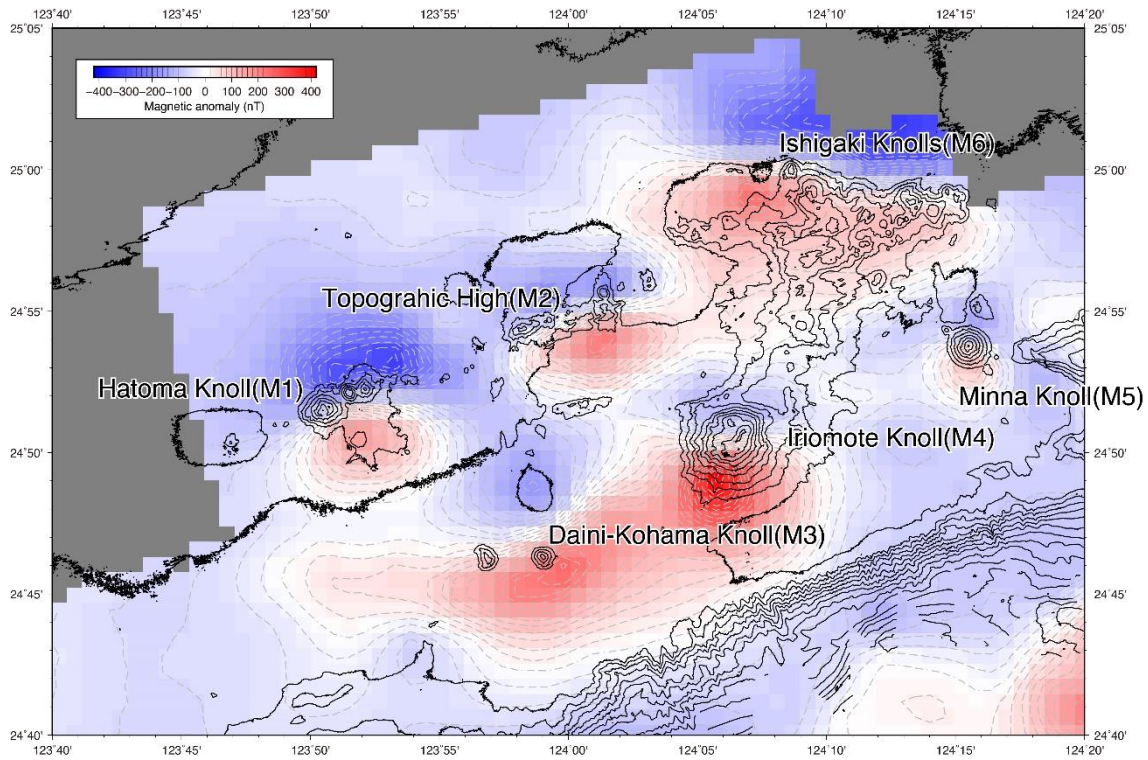
245 the wipe-out structure was recorded in the MBES data (Fig. S3e). This suggests that
246 some gas and/or fluid is emanating from the seafloor (e.g., Nakamura et al., 2015;
247 Miyazaki et al., 2017).

248

249 **Magnetic data**

250 A magnetic anomaly map (Fig. 5) shows clear dipole-shaped magnetic anomalies, or
251 pairs of negative and positive anomaly regions, in this region (M1–M6). The negative
252 regions of these anomalies are located to the north of the positive anomalies, indicating
253 that induced magnetizations and/or remnant magnetizations almost parallel to the
254 present field direction are the dominant source. Relative to bathymetry, all six
255 anomalies are distributed around the knolls; anomalies M1, M2, M3, M4, M5, and M6
256 are associated with Hatoma Knoll, topographic highs, Daini-Kohama Knoll, Iriomote
257 Knoll, Minna Knoll, and the Ishigaki Knolls, respectively. For magnetic anomalies that
258 originated from isolated dipole sources in the survey area, the interval between the
259 negative and positive anomaly peaks is nearly identical to the distance from the survey
260 plane to the dipole position. The negative-to-positive peak intervals for magnetic
261 anomalies M1–M5 have similar values from 3 to 7 km (M1: 4–5 km; M2: ~4 km; M3:
262 6–7 km; M4: 5–6 km; M5: ~3 km), suggesting that the source positions of these
263 anomalies assuming dipole sources, are located 3–7 km from the sea surface.
264 Considering the water depth of ~2 km in the survey area, the dipole sources are
265 probably located 1–5 km beneath the seafloor.

266



267

268 **Figure 5** Magnetic anomaly map offshore northern Ishigaki-Jima Island. The magnetic
 269 anomaly map grid interval is 1 km, and the contour interval is 20 nT. Dipole
 270 anomalies lie around the knolls, which are submarine volcano. They are
 271 characterized by a narrow interval between the positive and negative dipole
 272 anomalies. Bathymetry contours are shown as black lines. The bathymetry
 273 contour interval is 100 m.

274

275 **5. Discussion**

276 The graben identified in this study has developed by normal faulting and contains
 277 intrusive structures (Figs. 2 and 4). It resembles the Yaeyama Graben in the southern
 278 OT in terms of both bounding normal faults and intrusions (Lee et al., 1980; Arai et al.,
 279 2017). In the Bransfield Strait along the Antarctic Peninsula, where the continental
 280 margin backarc system is also in the rifting stage, a graben bounded by normal faults
 281 and a relatively homogeneous intrusion into the sedimentary basins have been observed

282 (Grad et al., 1992). A rift graben bounded by normal faults with several sills has been
283 documented in the Guaymas Basin in the Gulf of California, where seafloor spreading
284 has commenced (Lizarralde et al., 2007; Kluesner et al., 2014). The characteristics of
285 the graben identified in this study are similar to those of other rift grabens in different
286 stages of backarc system evolution in diverse tectonic settings.

287 Topographic highs with chaotic seismic characteristics are located along the axis of
288 the graben. We interpret these highs as submarine volcanos formed by magma extrusion
289 from the seafloor (Figs. 2 and 4). Dipole-shaped magnetic anomalies around Hatoma
290 Knoll (M1) and the topographic highs within the graben (M2) suggest the existence of
291 strong anomalous sources 2–3 km below the seafloor (Fig. 5). Such strong anomalous
292 sources at relatively shallow depths further support this interpretation. The gas and/or
293 fluid emanation on the north side of the graben may represent hydrothermal activity
294 associated with magmatism (Fig. S3). Shallow seismicity clusters with hypocenter
295 depths from 0 to 20 km along the graben indicates considerable seismic activity
296 around Hatoma Knoll and the topographic highs (Fig. 4a). It should be noted that the
297 accuracy of hypocenter locations in offshore areas is inferior to that for those on land
298 due to the limited number of seismic stations around the OT. These features and
299 characteristics suggest shallow magma as a heat source beneath the graben.

300 The southern margin of the OT is underlain by a heat source. Magma intrusion has
301 been recognized on the northwest side of the graben shown in this study (Fig.1b) (Arai
302 et al., 2017). The heat source is likely associated with the axial magma chamber below
303 the Yaeyama Rift (Fig. S4). Although more details of the structure should be
304 investigated by future geophysical surveys in the southern OT, the graben and
305 associated subseafloor structures can be regarded as embryonic rifting preceding
306 seafloor spreading. The features revealed in this study suggest that small-scale

307 magmatic activity and associated intrusive structures play an important role in the
308 development of normal faults, submarine volcanoes, and the graben in this early stage
309 of the backarc system.

310

311 **6. Conclusions**

312 Integrated marine geological and geophysical surveys incorporating high-density
313 survey lines were undertaken offshore northern Ishigaki-Jima Island. We identify a
314 graben bounded by normal faults off-axis of the southern OT. This graben extends ~59
315 km in the ENE-WSW direction. Submarine volcanoes such as Hatoma Knoll display
316 active hydrothermal activity, and associated intrusive structures lie within the graben.
317 The source depth of dipole-shaped magnetic anomalies and active seismicity shallower
318 than 20 km in and around the graben indicate relatively shallow magma acting as a heat
319 source. These features suggest active rifting in the graben, and that the graben likely
320 manifests embryonic rifting along the southern margin of the OT.

321

322 Acknowledgements

323 This study was conducted as a part of the “Geological Mapping Project Around the
324 Okinawa Islands” by the Geological Survey of Japan (GSJ) of National Institute of
325 Advanced Industrial Science and Technology (AIST). We are grateful to the captains
326 and crews of the R/V *Hakurei* and R/V *No.1 Kaiyo-Maru* for the professionalism they
327 displayed during the cruises. We are also indebted to the GK19 science party. We thank
328 Ryuta Arai for providing the location information on the location of the magma
329 chamber. In addition, we are deeply indebted to Prof. Mike Coffin and the anonymous
330 reviewer whose constructive comments and suggestions have improved our manuscript.

331 Most bathymetry was plotted using GMT software (Wessel and Smith,1991). The data
332 used in this paper are available online (<http://doi.org/10.6084/m9.figshare.11993520>).

333 **Reference**

- 334 Arai, K., Inoue, T., & Sato, T. (2018), High-density surveys conducted to reveal active
335 deformations of the upper forearc slope along the Ryukyu Trench, western Pacific,
336 Japan. *Progress in Earth and Planetary Science*, 5(1), 45.
- 337 Arai, R., Kodaira, S., Yuka, K., Takahashi, T., Miura, S., & Kaneda, Y. (2017), Crustal
338 structure of the southern Okinawa Trough: Symmetrical rifting, submarine volcano,
339 and potential mantle accretion in the continental back-arc basin. *Journal of*
340 *Geophysical Research: Solid Earth*, 122(1), 622-641.
- 341 Bouriak, S., Vanneste, M., & Saoutkine, A. (2000), Inferred gas hydrates and clay diapirs
342 near the Storegga Slide on the southern edge of the Vøring Plateau, offshore Norway,
343 *Marine Geology*, 163, 125-148.
- 344 DeMets, C., Gordon, R. G., & Argus, D. F. (2010). Geologically current plate motions.
345 *Geophysical Journal International*, 181(1), 1-80.
- 346 Dillon, W. P., Lee, M. W., Fehlhaber, K., & Coleman, D.F. (1993), Gas Hydrates on the
347 Atlantic Continental Margin of the. US Geological survey professional paper, (1570),
348 313., 313– 330
- 349 Grad, M., Guterch, A., & Janik, T. (1993), Seismic structure of the lithosphere across the
350 zone of subducted Drake plate under the Antarctic plate, West Antarctica. *Geophysical*
351 *Journal International*, 115(2), 586-600.
- 352 Hirata, N., Kinoshita, H., Katao, H., Baba, H., Kaiho, Y., Koresawa, S., Ono, Y. &
353 Hayashi, K. (1991), Report on DELP 1988 cruises in the Okinawa Trough: Part 3.
354 Crustal structure of the southern Okinawa Trough. *Bull. Earthquake Res. Inst. Univ.*
355 *Tokyo*, 66, 37-70.

356 Hornbach, M. J., Ruppel, C., & Van Dover, C. L. (2007), Three-dimensional structure of
357 fluid conduits sustaining an active deep marine cold seep, *Geophysical Research*
358 *Letters*, 34, L05601-05605.

359 Jourdain, A., Singh, S. C., Escartin, J., Klinger, Y., Raju, K. K., & McArdle, J. (2016),
360 Crustal accretion at a sedimented spreading center in the Andaman
361 Sea. *Geology*, 44(5), 351-354.

362 Keller, R. A., Fisk, M. R., Smellie, J. L., Strelin, J. A., & Lawver, L. A. (2002),
363 Geochemistry of back arc basin volcanism in Bransfield Strait, Antarctica: Subducted
364 contributions and along-axis variations. *Journal of Geophysical Research: Solid*
365 *Earth*, 107(B8), ECV-4.

366 Kizaki, K. (1986), Geology and tectonics of the Ryukyu
367 Islands. *Tectonophysics*, 125(1-3), 193-207.

368 Kluesner, J., Lonsdale, P., & González-Fernández, A. (2014), Late Pleistocene cyclicality
369 of sedimentation and spreading-center structure in the Central Gulf of California.
370 *Marine Geology*, 347, 58-68.

371 Konishi, K. (1965), Geotectonic Framework of the Ryukyu Islands (Nansei Shoto).
372 *Geological Journal*, 71, 437-457.

373 Konno, U., Tsunogai, U., Nakagawa, F., Nakaseama, M., Ishibashi, J. I., Nunoura, T., &
374 Nakamura, K. I. (2006), Liquid CO₂ venting on the seafloor: Yonaguni Knoll IV
375 hydrothermal system, Okinawa Trough. *Geophysical research letters*, 33(16).

376 Lee, C. S., Shor Jr, G. G., Bibee, L. D., Lu, R. S., & Hilde, T. W. (1980), Okinawa
377 Trough: origin of a back-arc basin. *Marine Geology*, 35(1-3), 219-241.

378 Letouzey, J. & Kimura, M. (1986), The Okinawa Trough: genesis of a back-arc basin
379 developing along a continental margin. *Tectonophysics*, 125(1-3), 209-230.

380 Lizarralde, D., Axen, G. J., Brown, H. E., Fletcher, J. M., González-Fernández, A.,
381 Harding, A. J., Holbrook, W.S., Knet, M. G., Paramo P., Sutherland, F., & Umhoefer,
382 P. J. (2007), Variation in styles of rifting in the Gulf of California. *Nature*, 448(7152),
383 466-469.

384 Nakahigashi, K., Shinohara, M., Suzuki, S., Hino, R., Shiobara, H., Takenaka, H.,
385 Nishino, M., Sato, T., Yoneshima, S., & Kanazawa, T. (2004), Seismic structure of the
386 crust and uppermost mantle in the incipient stage of back arc rifting—northernmost
387 Okinawa Trough. *Geophysical research letters*, 31(2).

388 Nakamura, K., Kawagucci, S., Kitada, K., Kumagai, H., Takai, K., & Okino, K. (2015),
389 Water column imaging with multibeam echo-sounding in the mid-Okinawa Trough:
390 Implications for distribution of deep-sea hydrothermal vent sites and the cause of
391 acoustic water column anomaly. *Geochemical Journal*, 49(6), 579-596.

392 Miki, M. (1995), Two-phase opening model for the Okinawa Trough inferred from
393 paleomagnetic study of the Ryukyu arc. *Journal of Geophysical Research: Solid*
394 *Earth*, 100(B5), 8169-8184.

395 Miyazaki, J., Kawagucci, S., Makabe, A., Takahashi, A., Kitada, K., Torimoto, J., Matsui,
396 Y., Tasumi, E., Sibuya, T., Nakamura, K., Horai, S., Sato, S., Ishibashi, J., Kanazaki,
397 H., Nakagawa, S., Hirai, M., Takaki, Y., Okino, K., Watanabe, K. H., Kumagai, H., &
398 Chan, C. (2017), Deepest and hottest hydrothermal activity in the Okinawa Trough: the
399 Yokosuka site at Yaeyama Knoll. *Royal Society open science*, 4(12), 171570.

400 Nishizawa, A., Kaneda, K., Oikawa, M., Horiuchi, D., Fujioka, Y., & Okada, C. (2019),
401 Seismic structure of rifting in the Okinawa Trough, an active backarc basin of the
402 Ryukyu (Nansei-Shoto) island arc–trench system. *Earth, Planets and Space*, 71(1), 21.

403 Raju, K. K., Ramprasad, T., Rao, P. S., Rao, B. R., & Varghese, J. (2004), New insights
404 into the tectonic evolution of the Andaman basin, northeast Indian Ocean. *Earth and*
405 *Planetary Science Letters*, 221(1-4), 145-162.

406 Sager, W. W., MacDonald, I. R., & Hou, R. S. (2003), Geophysical signatures of mud
407 mounds at hydrocarbon seeps on the Louisiana continental slope, northern Gulf of
408 Mexico, *Marine Geology*, 198, 97– 132.

409 Shipley, T. H., Moore, G. F., Bangs, N. L., Moore, J. C., & Stoffa, P. L. (1994),
410 Seismically inferred dilatancy distribution, northern Barbados Ridge decollement:
411 Implications for fluid migration and fault strength. *Geology*, 22(5), 411-414.

412 Sibuet, J. C., Letouzey, J., Barbier, F., Charvet, J., Foucher, J. P., Hilde, T. W., Kimura,
413 M., Chiao, L. Y., Marsset, B., Muller, C., & Stéphan, J. F. (1987), Back arc extension
414 in the Okinawa Trough. *Journal of Geophysical Research: Solid Earth*, 92(B13),
415 14041-14063.

416 Sibuet, J. C., Hsu, S. K., Shyu, C. T., & Liu, C. S. (1995), Structural and kinematic e
417 volutions of the Okinawa Trough backarc basin. In *Backarc basins* (pp. 343-379).
418 Springer, Boston, MA.

419 Sibuet, J. C., Deffontaines, B., Hsu, S. K., Thureau, N., Le Formal, J. P., & Liu, C. S.
420 (1998), Okinawa trough backarc basin: Early tectonic and magmatic
421 evolution. *Journal of Geophysical Research: Solid Earth*, 103(B12), 30245-30267.

422 Toki, T., Itoh, M., Iwata, D., Ohshima, S., Shinjo, R., Ishibashi, J. I., Tsunogai, U.,
423 Takahata, N., Sano, Y., Yamanaka, T., Ijiri, A., Okabe, N., Gamo, T., Muramatsu, Y.,
424 Ueno, Y., Kawagucci, S., & Takai, K. (2016), Geochemical characteristics of
425 hydrothermal fluids at Hatoma Knoll in the southern Okinawa Trough. *Geochemical*
426 *Journal*, 50(6), 493-525.

427 Watanabe, K., Shibata, A., Furukawa, H., & Kajimura, T. (1995), Topography of
428 submarine volcanoes off the North-Northeast Coast of Iriomote island, the Ryukyu
429 Islands. *Kazan*, 2(40), 91-97 (in Japanese).

430 Wessel. P., & Smith, W.H.F. (1991), Free software helps map and display data. *Eos*
431 *Trans AGU*, 72:441

432 Wessel. P. (2010), Tools for analyzing intersecting tracks: The x2sys package.
433 *Computers and Geosciences*, 72:441

434

435